Indoor Wireless Environment Visualization for Smart Factories

Hayato Mukasa*, Koshiro Aruga*, Takeo Fujii* and Koichi Adachi*
* Advanced Wireless and Communication Research Center (AWCC), The University of Electro-Communications
1–5–1 Chofugaoka, Chofu, Tokyo 182–8585, Japan
Emails: {mukasa, aruga, fujii, adachi}@awcc.uec.ac.jp

***Abstract*—Smart factories with a cyber-physical system (CPS) require wireless power transfer and data transmission for the CPS simultaneously without interference. For the design of these simultaneous transmissions, it is important to accurately recognize the wireless environment. One of the methods for recognizing the environment is a *radio environment map (REM)*, which visualizes the statistical results of measured received power and communication quality by linking them to location information. In this paper, we propose measuring the received power and communication quality of private 5G and wireless local area networks in a smart factory and constructing an indoor spectrum database. REMs were created from the constructed database and their accuracy was evaluated. We also compared the block error rate (BLER) and modulation and coding scheme (MCS) index at non-line-of-sight (NLOS) locations to those at LOS locations and found that MCS index decreased when BLER increased.**

I. Introduction

Industry 4.0 proposes the concept of smart factories to improve production efficiency in the manufacturing industry dramatically [1]. Smart factories can operate autonomously, with machines interconnected by an IoT platform and operating through a cyber-physical system (CPS). The CPS can provide optimal control for the physical domain through emulation on the cyber domain built by information on factory systems acquired in real-time through sensing. This control can enable full automation of high-mix, low-volume production, creating a smart factory with improved manufacturing flexibility, productivity, profitability, and safety [1]–[4].

To realize CPS in smart factories, it is necessary to place a huge number of sensors in physical space and aggregate the data in cyberspace with low latency. Aggregating data from numerous sensors requires a power source to operate the sensors and radio equipment. Wired power supply and batteries are commonly used to secure the power source. However, when there are numerous sensors, the wired power supply limits the installation location and wiring, and battery operation is impractical because of the time and effort required to replace the batteries.

Therefore, a power source using wireless power transfer (WPT) has been proposed [5], [6]. However, WPT interferes with nodes and sensor data transmission and prevents information aggregation. To minimize interference between information and WPT, as well as among users and systems that transmit information, it is important to accurately understand the wireless environment and allocate frequency resources.

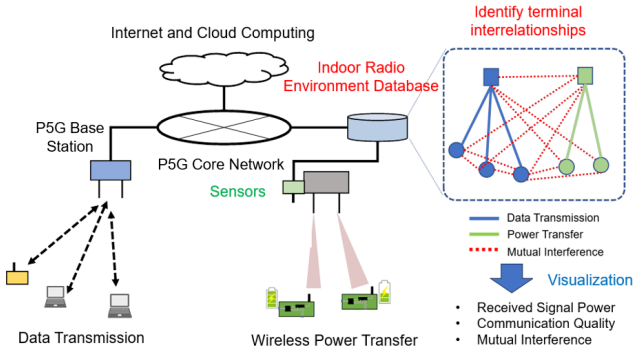

Fig. 1. Simultaneous transmission of data and power at the same frequency.

Nevertheless, analyzing indoor wireless environments, such as those in smart factories, remains challenging due to the impact of reflections and shadowing.

Hence, as a method to recognize the wireless environment with high accuracy, utilizing a spectrum database that accumulates information observed from nodes and makes it into statistics has been proposed. As use cases of the spectrum database, a radio environment map (REM) that visualizes the radio propagation environment by mapping the statistical results of measured received power related to location information and a frequency management method based on the measured data have been proposed [7]–[9].

In this study, we proposed and created an indoor spectrum database by accumulating measured received power and communication quality in a smart factory. Using this database, REMs were created to visualize the radio propagation environment. In addition, the relationship between block error rate (BLER) and modulation and coding scheme (MCS) index was investigated to improve the predictability of communication quality prediction.

II. Indoor Spectrum Database

As a method to recognize the wireless environment with high accuracy, the method using a spectrum database that makes statistics through collected measurement data from nodes has been proposed [7]–[9]. This section describes purposes of an indoor spectrum database in a smart factory and explains the construction process of the database.

Fig.1 shows an indoor spectrum database and simultaneous transmission of information and power in a smart factory. In a smart factory, it is better to use the same frequency

on simultaneous transmission of information and power for improving spectrum efficiency. Nodes and sensors operating in the smart factory perform information transmission with Private 5G (P5G), while WPT is performed on sensors and other devices that perform sensing. The proposed indoor spectrum database is connected to the P5G core network and devices that perform WPT to collect data. Based on the collected information, the indoor spectrum database can be used for designing simultaneous transmission of information and power by visualizing the received signal power, communication quality, and mutual interference.

III. Measurement Campaign

A. Measurement Overview

Received power and communication quality were measured in a smart factory for the construction of an indoor spectrum database. P5G and Wireless local area network (WLAN) access points (APs) were placed at the same location in the Learning Factory (LF) of the Okayama R&D Center of Yamamoto Metal Technos, and measurements were performed. The LF is a factory that conducts demonstration experiment to realize a smart factory. The layout of the LF is shown in Fig. 2. The observation area in the LF was meshed into a 1 [m] × 1 [m] area, and received power and communication quality were measured using multiple observation devices placed on the container as shown in Fig. 3. The measurement environment is shown in Fig. 4, where countless devices are installed and there are many metallic objects as obstacles.

As shown in Fig. 2, the P5G base station (BS) was installed in a room adjacent to the measurement area. Two WLAN APs were also installed at the same location as the P5G BS. The WLAN APs used were a TP-Link AX5400 with six antennas and a TP-Link AC750 with one antenna.

Table I shows the measurement specifications. First, the received power of the WLAN was measured in the LF using three smartphones. One and six antennas were used at WLAN APs, and measurements were performed at 2.4 GHz and 5 GHz for each AP, respectively. The measurement equipment in Fig. 3 was placed at the center of each mesh, and the received signal strength indicator (RSSI) was collected at each terminal every 1 second for 40 seconds using three smartphones. In each mesh, a total of 120 data sets were used to create REMs.

Then, the received power and communication quality of P5G were measured in the LF. For the P5G measurement, a network scanner (PCTEL IBflex) supporting 5G/private 5G was used as the measurement equipment. In addition, measurements were conducted simultaneously using a KYOCERA 5G router (K5G-C-100A) and XCAL, a wireless network observation tool. XCAL can obtain various communication metrics and parameters related to 5G, such as BLER, number of resource blocks, and MCS index.

PCTEL IBflex measured the synchronization signal-reference signal received power (SS-RSRP), which is the received power per resource element of the SS-Block synchronization signal in the 5G Sub-6 signal. In the measurement using XCAL, an iperf server was connected to the BS, and

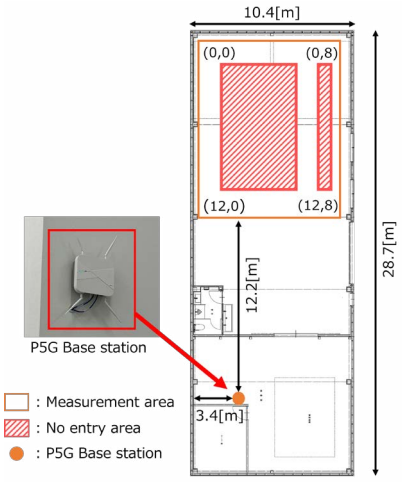

Fig. 2. Layout of LF.

Fig. 3. Measuring instruments.

Fig. 4. Measurement environment.

traffic was applied to obtain information about 5G such as RSRP, BLER, and MCS index using XCAL. The P5G measurements were made for 60 seconds, with PCTEL IBflex using approximately 2000 data points to create REMs and XCAL using 60 data points to create REMs.

B. Creation of REM

REMs were created based on the measured received power in WLAN and P5G. The received power at each mesh of REMs was averaged and used as the representative value for that mesh. To verify the accuracy of the REM, the root mean squared error (RMSE) for each mesh and the RMSE for the entire REM were derived.

The RMSE at mesh k is expressed as

$$RMSE_k = \sqrt{\frac{1}{n_k}\sum_{i=1}^{n_k}(P_{k,i} - \hat{P}_k)^2}, \tag{1}$$

where n_k is the number of data measured in the mesh k, $P_{k,i}$ is the ith instantaneous received power [dBm] in mesh k , and $\hat{P}_k$ is the average received power [dBm] in mesh k.

On the other hand, the RMSE of the entire REM is expressed as

$$RMSE_{all} = \sqrt{\frac{1}{mn_k}\sum_{k=1}^{m}\sum_{i=1}^{n_k}(P_{k,i} - \hat{P}_k)^2}, \tag{2}$$

where m is the number of meshes, $P_{k,i}$ is the ith instantaneous received power [dBm] in mesh k, and $\hat{P}_k$ is the average received power [dBm] in mesh k.

TABLE I
MEASUREMENT SPECIFICATION.

P5G or WLAN	Num. of BS/AP antennas	Meas. equip.	Center freq. [MHz]
P5G	4	Network scanner (PCTEL Ibflex)	4849.86
P5G	4	Router (K5G-C-100A) + Measurement Software (XCAL)	4849.86
WLAN [TP-Link AX5400]	6	Oppo A55s ×1 Zenfone 7 ×2	2412
WLAN [TP-Link AX5400]	6	Oppo A55s ×1 Zenfone 7 ×2	5240
WLAN [TP-Link AX750]	1	Oppo A55s ×1 Zenfone 7 ×2	2412
WLAN [TP-Link AX750]	1	Oppo A55s ×1 Zenfone 7 ×2	5240

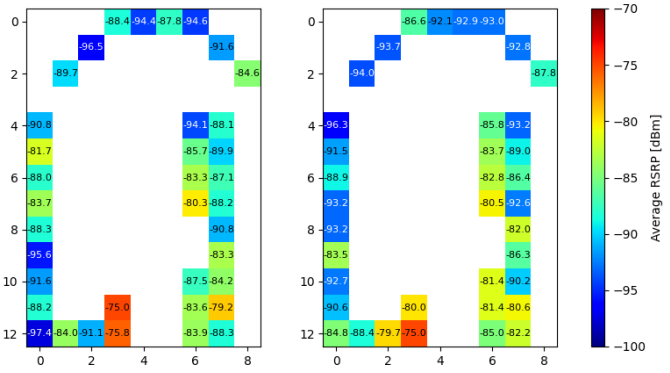

Fig. 5. P5G REM for downlink(left) PCTEL IBflex (right) XCAL.

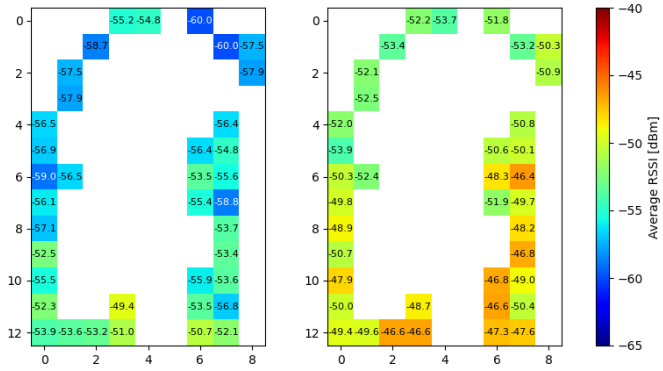

Fig. 6. WLAN REM for 2.4[GHZ](left) 1 antenna (right) 6 antennas.

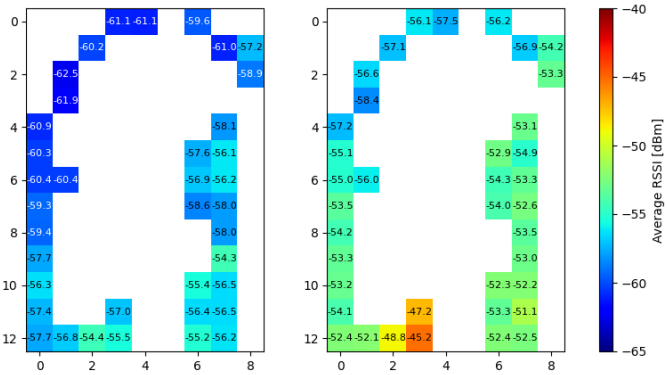

Fig. 7. WLAN REM for 5[GHZ](left) 1 antenna (right) 6 antennas.

IV. MEASUREMENT RESULTS AND ANALYSIS

In this section, the REM prepared based on the radio environment information collected by the measurement campaign and its accuracy are shown. As an examination of the communication quality index stored in the indoor spectrum database, MCS index and BLER obtained by the measurement of P5G are compared.

A. Radio Environment Map

While downlink (DL) and uplink (UL) REMs were constructed for the P5G measurements, this paper shows the DL results. Fig. 5 shows the REMs for P5G DL communications. The representative value of the mesh in Fig. 5 is the average RSRP. Figs. 6 and 7 show the REMs of the wireless LAN at 2.4 [GHz] and 5 [GHz], respectively. The representative value of the mesh in Fig. 6 and 7 is the average RSSI. Figs. 6 and 7 show that the AP with 6 antennas tends to have a higher average RSSI overall than the AP with 1 antenna, and 2.4 GHz is less affected by distance attenuation. Note that x and y in mesh (x,y) represent the vertical and horizontal axes of the REM, respectively.

Next, the accuracy of the created REM is evaluated. Figs. 8 and 9 show the Cumulative Distribution Function (CDF) of the RMSE of the REM in P5G and WLAN. In addition, Table II and III show the RMSE of all meshes of the REMs in P5G and wireless LAN. From Fig. 8 and Table II, the average and worst values of the RMSE of the REM of P5G are lower than those of the REM of wireless LAN, and it can be said that the accuracy of the REM of wireless LAN is worse. It is considered that the reason is that the REM is created by averaging the values of three nodes, while in the case of P5G, only one measuring instrument is used.

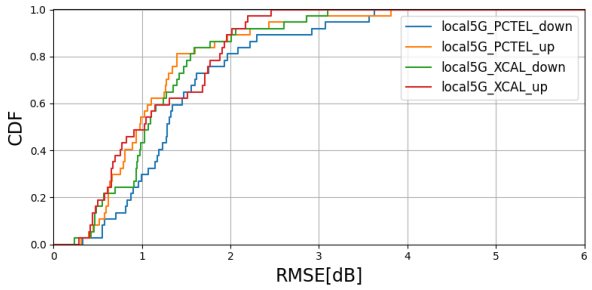

Fig. 8. CDF of RMSE of P5G.

TABLE II
RMSE OF THE ENTIRE REM IN P5G.

DL/UL	Meas. equip.	Center Freq.[MHz]	Meshes' RMSE[dB]
DL	PCTEL	4849.86	1.677
UL	PCTEL	4849.86	1.378
DL	XCAL	4849.86	1.393
UL	XCAL	4849.86	1.324

B. Analysis of Communication Quality Indicators

The proposed indoor spectrum database also aims to visualize communication quality. Hence, we considered the

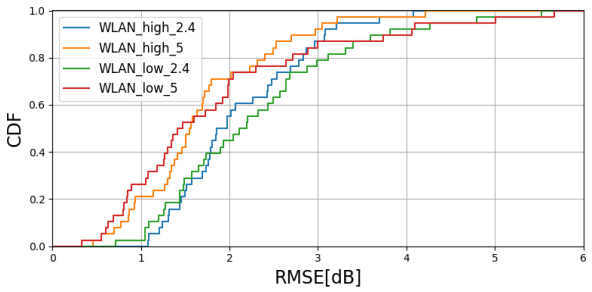

Fig. 9. CDF of RMSE of WLAN.

TABLE III
RMSE OF THE ENTIRE REM IN WLAN.

Num. of AP's antennas	Center freq. [MHz]	Meshes' RMSE [dB]
1	2412	2.553
1	5240	2.246
6	2412	2.239
6	5240	1.885

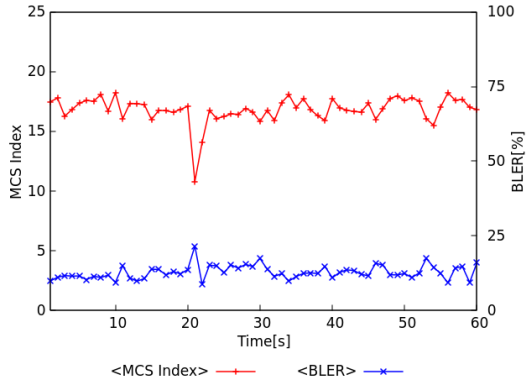

Fig. 10. Relationship between MCS and BLER in P5G DL: Mesh(1,7).

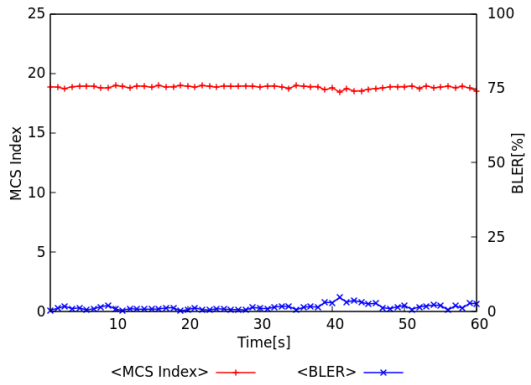

Fig. 11. Relationship between MCS and BLER in P5G DL: Mesh(11,3).

indicators of communication quality to be stored in the indoor spectrum database. In the P5G measurement campaign, using XCAL, we measured several values that could be indicators of communication quality. In this paper, we focus on MCS, which represents a combination of modulation method and coding rate, and BLER, which represents communication quality, for analysis.

The BLER and MCS for DL communication at mesh (1,7) and (11,3) are shown in Fig. 10 and Fig. 11, respectively. The left vertical axis in Figs. 10 and 11 shows the average value of the MCS index at unit time, the right vertical axis shows the BLER at unit time, and the horizontal axis shows the time passage. The mesh (1, 7) is non-line-of-sight (NLOS) and the mesh (11, 3) is line-of-sight (LOS) environments. According to Fig. 10, at mesh (11,3), which is a LOS environment, BLER is stable at a low value and MCS is also stable. On the other hand, Fig. 10 shows that at mesh (1,7), which is an NLOS environment, BLER is higher and more variable than at mesh (11,3), and MCS values are also more volatile. Focusing on the time point from 20 to 21 seconds in Fig. 10, BLER is increasing while MCS is decreasing from about 18 to 11. The above suggests that when the quality of the channel degrades (BLER increases), MCS decreases.

V. CONCLUSIONS AND FUTURE WORK

In this paper, we proposed to construct an indoor spectrum database to understand the wireless environment in a smart factory. The indoor wireless environment was successfully visualized by measuring the received power of wireless LAN and private 5G which are a kind of private network, and creating a REM. In addition to the received power measurements, the private 5G also measured BLER and MCS, confirming the decrease in MCS index due to degraded channel conditions.

Future work will include a selection of information to be stored in the indoor spectrum database. Consideration will be given to indicators that correlate with throughput, BLER, etc.

ACKNOWLEDGMENT

This study was supported by National Institute of Information and Communications Technology (NICT), Japan (JPJ012368C07301).

REFERENCES

[1] P. A. Okeme, A. D. Skakun and A. R. Muzalevskii, "Transformation of factory to smart factory," In *Proc. IEEE Conf. Russian Young Researchers in Elect. and Electron. Eng. (ElConRus)*, pp.1499–1503, Jan. 2021.

[2] T. Tanagi and K. Adachi, "Dynamic path planning for QoS improvement in multiple automated guided vehicles," *2023 VTS Asia Pacific Wireless Commun. Symp. (APWCS)*, pp.1–5, 2023.

[3] F. Ohori, S. Itaya, T. Osuga and F. Kojima, "Estimating wireless link quality using multiple remote sensors for wireless control of AGV in a factory," *Proc. 2020 23rd Int. Symp. on Wireless Pers. Multimedia Commun. (WPMC)*, pp.1–6, Oct. 2020.

[4] W. Xia, J. Goh, C. A. Cortes, Y. Lu and X. Xu, "Decentralized coordination of autonomous AGVs for flexible factory automation in the context of Industry 4.0," *Proc. 2020 IEEE 16th Int. Conf. on Automation Science and Eng. (CASE)*, pp.488–493, Aug. 2020.

[5] Z. Zhang, H. Pang, A. Georgiadis and C. Cecati, "Wireless power transfer — an overview," in *IEEE Tran. on Ind. Electronics*, vol.66, no.2, pp.1044–1058, Feb. 2019.

[6] M. Sugino and T. Masamura, "The wireless power transfer systems using the Class E push-pull inverter for industrial robots," in *Proc. Wireless Power Transfer Conf. (WPTC)*, pp.1–3, 2017.

[7] S. Bi, J. Lyu, Z. Ding and R. Zhang, "Engineering radio maps for wireless resource management," in *IEEE Wireless Commun.*, vol.26, no. 2, pp.133–141, April 2019.

[8] S. Yamada, T. Fujii, K. Suto and K. Sato, "Observation data and 3D map-based radio environment estimation for drone wireless communications," *2023 Fourteenth Int. Conf. on Ubiquitous and Future Networks (ICUFN)*, pp. 70–75, 2023.

[9] H. R. Imam, K. Inage, M. Ohta and T. Fujii, "Measurement based radio environment database using spectrum sensing in cognitive radio," *Proc. Int. Conf. Sel. Topics Mobile Wireless Netw. (iCOST)*, pp. 110–115, Oct. 2011.